NASA TECHNICAL TRANSLATION NASA TT F-14,288

CALCULATION OF THE PROPERTY OF EXPANSION CHAMBER TYPE MUFFLERS

J. Okda

Details of illustrations in this document may be better studied on microfiche

Source: Journal of Acoustical Society of Japan, Vol. 25, No. 3, pp. 122-29, 1969.

(NASA-TT-F-14288) CALCULATION OF THE PROPERTY OF EXPANSION CHAMBER TYPE MUFFLERS J. Okda (Scientific Translation Service) Jul. 1972 17 p CSCL 20A

N72-26554

Unclas G3/23 33376

NATIONAL AERONAUTICS AND SPACE ADMINISTRATION
WASHINGTON, D. C. 20546 JULY 1972

Reproduced by
NATIONAL TECHNICAL INFORMATION SERVICE
U S Department of Commerce
Springfield VA 22151

17p

CALCULATION OF THE PROPERTY OF EXPANSION CHAMBER TYPE MUFFLERS*

Josuke Okda**

ABSTRACT. To express the noise reducing effect of a muffler in terms of the difference in the sound power levels radiated from the tailpipe exit with and without the muffler in the system, equations are deduced by means of the four-terminal constants (A B C D) of the equivalent electrical network of the whole muffler system.

The results are shown in Figures 7 and 8. Measured curves are in good agreement with those obtained by graphical methods so far as the sound wave in the chamber can be regarded as a plane wave. In the higher frequency range above the lowest resonance frequency in the direction perpendicular to the axis of the chamber, the sound wave can not be regarded as a plane wave, and noise reduction may not be expected.

1. Introduction

In spite of extensive research on expansion-type /123** muffler systems, other than TL, there are no publications on practical mathematical expressions for them.

The effectiveness of the muffler system should be evaluated in terms of the reduction in externally radiated sound power. For this purpose, it is insufficient to simply only

*Received November 27, 1968.

**Faculty of Engineering, Kumamoto University.

***Numbers in the margin indicate pagination in the original foreign text.

consider the TL of the chamber; it is necessary to consider the sound source impedance, the length of the input pipe, the length of the tailpipe, radiation impedance, etc.

From this point of view, a new mathematical expression was derived and the study of its practicality was conducted.

2. Muffler System Characteristics

When the noise from a noise source is radiated externally through a duct, the sound pressure level at a given point is determined by the radiated sound power level at the duct outlet and the directivity of the outlet to the given point, providing the external conditions are uniform [1].

If it is assumed that the input to the duct can be treated as an analogous acoustic circuit, and when the capability of the noise source to generate the noise is represented by an effective pressure p_0, and its source impedance — by $RZ_0 = jX_0$*, the maximum sound power generated by the noise source is [2]

$$W_0 = \frac{\overline{p_0^2}}{4R_0} \tag{1}$$

When the radiated power at the outlet of the duct is W_2, the change in the radiated power with the muffler system incorporated is

$$\frac{W_2'}{W_2} = \frac{W_0}{W_2} \cdot \frac{W_2'}{W_0} \tag{2}$$

where the primed parameters denote the values without the muffler system. It can be said that the purpose of the muffler system is to increase W_0/W_2.

*Translator's note: This should be $Z_0 = R + jX_0$.

When the power out of the noise source and to the duct is W_1, then,

$$\frac{W_0}{W_2}=\frac{W_0}{W_1}\cdot\frac{W_1}{W_2} \qquad (3)$$

The objective of an absorption-type muffler system is to increase W_1/W_2 and the purpose of the reactance-type muffler system is to increase W_0/W_1, since $W_1 = W_2$. It can be said that the latter system mismatches the sound source and the duct impedances.

If the duct outlet can also be treated as an analogous acoustic circuit, the radiation impedance is $Z_2 = R_2 + jX_2$. When the sound source reactance X_0 and the radiation reactance X_2 are included as a part of the duct, and if the length is handled strictly as an equivalent length, the equivalent circuit between the noise source and the duct outlet can be written as shown in Figure 1. The parameter p_1 is the sound pressure across the equivalent duct input impedance $Z_{11} = R_{11} + jX_{11}$ (including X_0), and p_2 is the sound pressure across R_2. In addition, U_1 is the volume velocity of the sound source, U_2 is that of the outlet, and the change, also expressed in terms of p_0, shows the basic effectiveness of the muffler system.

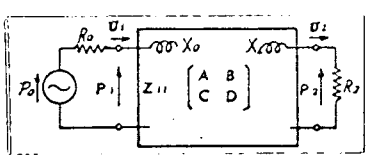

Figure 1. Equivalent electrical network of a muffler system. $R_0 + jX_2$: the internal impedance of the source, $R_2 + jX_2$: the radiation impedance of the tailpipe exit

When the four-terminal constant of the duct equivalent circuit is taken as ABCD,

$$\begin{bmatrix} p_1 \\ U_1 \end{bmatrix}=\begin{bmatrix} A & B \\ C & D \end{bmatrix}\begin{bmatrix} p_2 \\ U_2 \end{bmatrix} \qquad (4)$$

$$p_0=U_1 R_0+p_1 \qquad (5)$$

$$p_2=U_2 R_2 \qquad (6)$$

and

$$p_0=(R_0+Z_{11})(CR_2+D)U_2 \tag{7}$$

$$Z_{11}=\frac{p_1}{U_1}=\frac{AR_2+B}{CR_2+D} \tag{8}$$

Hence, Equation (3) can be derived as follows:

$$\frac{W_0}{W_2}=\frac{p_0^2/4R_0}{|U_2|^2R_2}=\frac{|R_0+Z_{11}|^2|CR_2+D|^2}{4R_0R_2} \tag{9}$$

3. Characteristic Equation for Expansion-Type Muffler System

Figure 2 illustrates the configuration of a simple expansion-type muffler system using a single basic chamber, with an input pipe, a chamber, and a tailpipe. The following assumptions are made in calculating its properties:

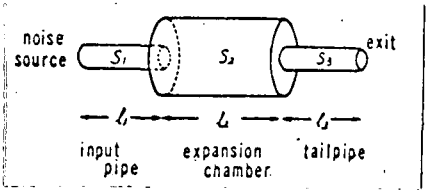

Figure 2. Schematic view of an expansion chamber type muffler

/124

(1) The sound pressure is considerably smaller than the average pressure in the duct.

(2) The duct medium is uniform; medium density ρ and the speed of sound c are constant.

(3) The wall surface does not vibrate; it is acoustically rigid and there is no transmission or absorption of sound energy.

(4) Effects of medium viscosity can be neglected.

(5) Effects of air current can be neglected.

(6) The sound wave in the tubular part, including the tubular chamber, is an axially-propagating plane wave.

Based on Assumption (1), the phenomenon is in alignment, and from (6), it is appropriate to assume that the cross section of the input pipe, as well as the tail pipe — with their respective cross-sectional areas smaller than that of the chamber — is considerably smaller than the wavelength, and it is possible to handle the cross section in terms of its equivalent acoustic circuit. In addition, it can be considered that the output radiation resistance R_2 is considerably smaller than the characteristic impedance of the tailpipe.

The true value of the source resistance R_0 generally is not only difficult to determine, but when it is discretional, the mathematical expression can become complex and, therefore, impractical. Hence R_0 will be represented by a constant-pressure source (in such cases when the sound leaks through the crack in the wall) or when it is smaller than $|Z_{11}|$ or, conversely, by a constant-velocity source (such as internal combustion engine or blower) when it is larger than $|Z_{11}|$. Since R_2 is small, except when $|B|$ and $|D|$ are extremely small (this is where the muffler system is ineffective), Equation (9) becomes

$$\frac{W_0}{W_2}\simeq\frac{1}{4R_0R_2}|B|^2 \quad \text{(Constant Pressure Source)} \tag{10}$$

$$\frac{W_0}{W_2}\simeq\frac{R_0}{4R_2}|D|^2 \quad \text{(Constant Velocity Source)} \tag{11}$$

Therefore, from Equation (2) the effectiveness of the muffler system can be shown as

$$L=L_i-L_i'+10\log\frac{R_2'}{R_2}\ [\mathrm{dB}] \tag{12}$$

$$L_i=20\log\frac{|B|}{Z_1},\quad L_i'=20\log\frac{|B'|}{Z_1} \quad \text{(Constant-Pressure Source)} \tag{13}$$

$$L_i=20\log|D|,\quad L_i'=20\log|D'| \quad \text{(Constant-Velocity Source)} \tag{14}$$

The primed parameters are those without the muffler system. Because B has a dimension in impedance, it is made dimensionless by dividing the characteristic impedance Z_1 of the input pipe.

The value of 10 log R_2'/R_2 is 0 when the outlet condition does not change with the use of the muffler system (that is, it is an opening in the wall, or is projected into space). It is 3 dB when the condition changes from one with an opening in the wall to that projected into space; and − 3 dB for the opposite change [2].

For the muffler system of Figure 2, with the cross-sectional area of the various parts as S_1, S_2, and S_3, and with the normalized equivalent length as l_1, l_2, and l_3,

$$\begin{aligned} B = jZ_1\{&\sin kl_1\cos kl_2\cos kl_3 \\ &+m_{12}\cos kl_1\sin kl_2\cos kl_3 \\ &+m_{13}\cos kl_1\cos kl_2\sin kl_3 \\ &-m_{23}\sin kl_1\sin kl_2\sin kl_3\} \end{aligned} \tag{15}$$

$$\begin{aligned} D = &\cos kl_1\cos kl_2\cos kl_3 \\ &-m_{12}\sin kl_1\sin kl_2\cos kl_3 \\ &-m_{13}\sin kl_1\cos kl_2\sin kl_3 \\ &-m_{23}\cos kl_1\sin kl_2\sin kl_3 \end{aligned} \tag{16}$$

where k is the wavelength constant, $Z_i = \rho c/S_i$ ($i = 1, 2, 3$) is the characteristic impedance, and

$$m_{ij} = \frac{Z_j}{Z_i} = \frac{S_i}{S_j} \tag{17}$$

When S_2 is considerably larger than S_1 or S_3, and when terms other than that with the highest-ordered cross-sectional area ratio m_{23} are neglected,

$$B \simeq (jZ_1\sin kl_1)\left(j\frac{1}{Z_2}\sin kl_2\right)(jZ_3\sin kl_3) \tag{18}$$

$$D \simeq (\cos kl_1)\left(j\frac{1}{Z_2}\sin kl_2\right)(jZ_3\sin kl_3) \tag{19}$$

The term $jZ_i \sin kl_i$ of the above equation is the ratio of the open-pipe input sound pressure and the output volume velocity (in equivalent circuit, the short-circuit transmission impedance); $\cos kl_i$ is the ratio of the open-pipe input and output volume velocities (the propagation constant), and $j(1/Z_2) \sin kl_2$ is the ratio of the open-pipe input volume velocity and the output sound pressure (in equivalent circuit, the open-circuit transmission admittance). In other words, various parts of the muffler system can be analyzed separately as shown in Figure 3 with their outlet opened when opened to a large area such as a chamber of external space, or closed when it is a narrow opening. Each part can be analyzed independently and the resultant can then be synthesized by summing the responses of each part.

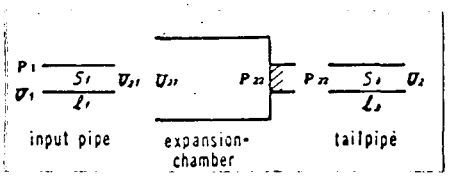

Figure 3. Elements of the expansion chamber type muffler

When the equivalent open-circuit transmission admittance of the chamber is expressed as Y_f, in general, /125

$$L_t = 20\log|\sin kl_1| + 20\log|Y_f Z_3| + 20\log|\sin kl_3| \quad \text{(Constant-Pressure Source)} \tag{20}$$

$$L_t = 20\log|\cos kl_1| + 20\log|Y_f Z_3| + 20\log|\sin kl_3| \quad \text{(Constant-Velocity Source)} \tag{21}$$

The term $20 \log |Y_f Z_3|$ expresses the properties of the chamber, and Table 1 lists the result of the calculations made for several types of chambers.

When kl_1 is small, Equations (18) and (19) cannot be approximated. In this range, it can be handled as a lumped constant

TABLE 1. 20 log $|Y_f Z_3|$ OF CYLINDRICAL CHAMBERS

expansion chamber	$20\log\|Y_f Z_3\|$ (dB)	curve (f : linier scale)
1. basic type 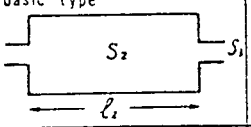	$20\log m_{23} + 20\log\|\sin k l_2\|$ $(m_{23} = S_2/S_3)$	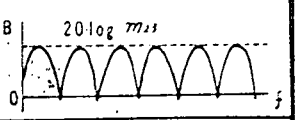
2-1. insert-pipe type 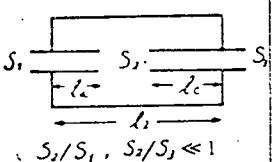 S_2/S_1, $S_2/S_3 \ll 1$	general form $20\log m_{23} + 20\log\|\sin k l_2\| - 20\log\|\cos k l_a\| - 20\log\|\cos k l_c\|$	
	(a) one of $(l_a, l_c) = 0$, the other $= l_2/2$ $20\log m_{23} + 6 + 20\log\|\sin k\frac{l_2}{2}\|$	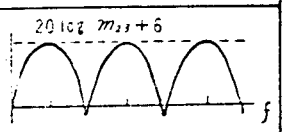
	(b) one of $(l_a, l_c) = 0$, the other $= l_2/4$ $20\log m_{23} + 12 + 20\log\|\sin k\frac{l_2}{4}\| + 20\log\|\cos k\frac{l_2}{2}\|$	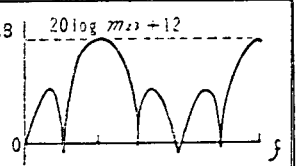
2-2. side-pipe type 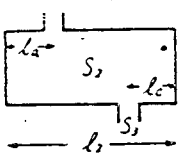	(c) one of $(l_a, l_c) = l_2/2$, the other $= l_2/4$ $20\log m_{23} + 12 + 20\log\|\sin k\frac{l_2}{4}\|$	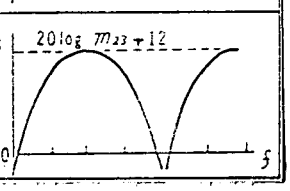

element; the type of chamber is immaterial. Equations (20) and (21) therefore become [2]

$$L_t = 20\log k l_1 + 20\log\left|1 + \frac{l_3 S_1}{l_1 S_3} - (k l_3)^2 \frac{V}{l_3 S_3}\right| \quad \text{(Constant-Pressure Source)} \tag{22}$$

$$L_t = 20\log\left|1 - (k l_3)^2 \frac{V}{l_3 S_3}\right| \quad \text{(Constant-Velocity Source)} \tag{23}$$

Reproduced from best available copy.

where V is its volume.

For more than two chambers, a similar analysis and calculation can be used. In the case of two chambers — when the equivalent open-circuit transmission admittance of the chambers is Y_{f1} and Y_{f2}, the volume is V_1 and V_2, the cross-sectional area

of the duct that connects the two chambers is S_d, the characteristic impedance is $Z_d = \rho c/S_d$, and the equivalent length is l_d — the resultant property of the two cavities is

$$\left.\begin{aligned} 20\log|Y_f Z_3| = {} & 20\log|Y_f Z_d| \\ & + 20\log|\sin k l_d| \\ & + 20\log|Y_f Z_3| \end{aligned}\right| \qquad (24)$$

In the low frequency range, the system must be handled in terms of lumped constant elements similar to the case of a single chamber. That is, for the two-chamber case when $S_1 = S_d = S_3$,

$$\left.\begin{aligned} L_r = {} & 20\log k l_1 + 20\log\left|\left\{1-(k l_d)^2\frac{V_1}{l_d S_d}\right\}\times\right. \\ & \times\left\{1-(k l_3)^2\frac{V_2}{l_3 S_3}\right\}+\frac{l_d}{l_1}+\frac{l_3}{l_1} \\ & \left.-(k l_3)^2\frac{V_1}{l_3 S_3}\left(1+\frac{l_d}{l_1}\frac{V_2}{V_1}\right)\right| \end{aligned}\right|$$

(Constant-Pressure Source) (25)

$$\left.\begin{aligned} L_r = {} & 20\log\left|\left\{1-(k l_d)^2\frac{V_1}{l_d S_d}\right\}\times\right. \\ & \left.\times\left\{1-(k l_3)^2\frac{V_2}{l_3 S_3}\right\}-(k l_3)^2\frac{V_1}{l_3 S_3}\right| \end{aligned}\right|$$

(Constant-Velocity Source) (26)

/126

Table 2 lists the values of 20 log $|Y_f Z_3|$ for a number of examples. In the case of numerous chambers, the length of the various sections must be adequately represented or else the effects cannot be achieved in relative proportion to the number of sections.

Moreover, although the value prior to the installation of the muffler system can be similarly calculated, the most general type is the case of one duct. When the cross-sectional area is S' and the equivalent length is l', we have

$$L_r' = 20\log|\sin k l'| + 20\log\frac{S_1}{S'} \quad \text{(Constant-Pressure Source)} \qquad (27)$$

$$L_r' = 20\log|\cos k l'| \quad \text{(Constant-Velocity Source)} \qquad (28)$$

TABLE 2. 20 log $|Y_f Z_3|$ OF COMBINED CHAMBERS

expansion chamber	$20\log\lvert Y_f Z_3\rvert$ (dB)	curve (f : linier scale)
3-1 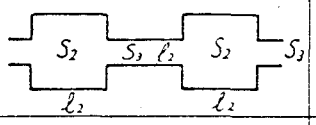	$40\log m_{23} + 60\log\lvert\sin k\ell_2\rvert$ $(m_{23}=S_2/S_3)$	(dotted curve – one chamber) 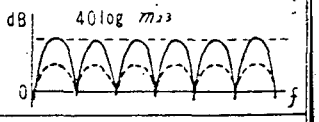
3-2 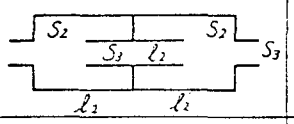	$40\log m_{23} + 12 + 40\log\lvert\sin k\frac{\ell_2}{2}\rvert$ $+20\log\lvert\sin k\ell_2\rvert$	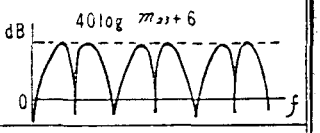
3-3 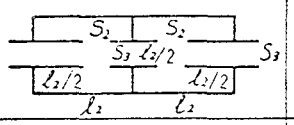	$40\log m_{23} + 24 + 40\log\lvert\sin k\frac{\ell_2}{4}\rvert$ $+20\log\lvert\sin k\frac{\ell_2}{2}\rvert$	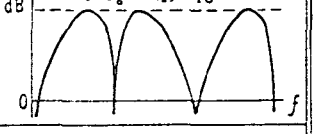
3-4 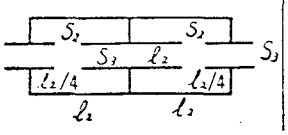	$40\log m_{23} + 24 + 40\log\lvert\sin k\frac{\ell_2}{4}\rvert$ $+20\log\lvert\sin k\ell_2\rvert$	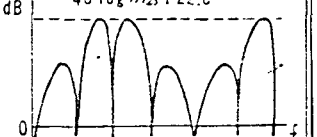

Reproduced from best available copy.

4. Graphical Determination of the Result

The plot of 20 log $|Y_f Z_3|$ and of Equations (12), (20), and (21), etc., as shown in Tables 1 and 2, can be easily obtained by a graphical method without performing numerical calculations [3].

First of all, prepare a plot of 20 log |sin x| and 20 log |cos x| using graph paper with the abscissa in logarithmic scale and the ordinate in a dB scale. The plot of 20 log $|\sin k\ell_i|$ and 20 log $|\cos k\ell_i|$ is obtained by sliding the location of x = 1 of the above plot such that it coincides with that of a frequency with $k\ell_i = 1$. In addition, their peaks and nulls can also be found graphically from the peaks and nulls of the above plots. Moreover, for the low frequency range, L_s makes use of a plot of such equations as Equations (22) and (23).

An example of the procedure in obtaining the composite property is shown in Figure 4.

5. Experimental Evaluation

The equipment shown in Figure 5 was used to experimentally obtain the value of 20 log $|Y_f Z_3|$. As in Figure 3, when the input pipe and the chamber are analyzed independently and approximated,

$$\frac{p_1}{p_{22}} = \frac{p_1}{U_{21}} \cdot \frac{U_{21}}{p_{22}} \simeq jZ_1 \sin k l_1 \cdot Y_f \qquad (29)$$

and therefore,

$$\begin{aligned} 20\log|Y_f Z_3| = {} & 20\log|p_1| - 20\log|p_{22}| \\ & + 20\log m_{13} \\ & - 20\log|\sin k l_1| \end{aligned} \qquad (30)$$

The first two terms are obtained from measurements, and the latter two — by calculation. The value of p_1 is fed back to provide a constant-pressure source. When $|p_{22}|$ is recorded on a recorder, the plot of 20 log $|Y_f Z_3|$ can be easily synthesized graphically (on recorder paper) because 20 log $|p_1|$ and 20 log m_{13} are fixed magnitudes. In this case, the fact must be considered that losses that were neglected theoretically do exist, though insignificantly, and that nulls of 20 log $|\sin k l_1|$, due to approximations, do have finite values. Furthermore, for the low frequency range, although resonance results due to interaction between the input pipe and the chamber, in this range $Y_f = j\omega V/\rho c^2$. When they are developed into a muffler system, there is no need for measurement because the system must be calculated as a lumped constant element. A 30-watt horn speaker unit was used for the speaker.

/127

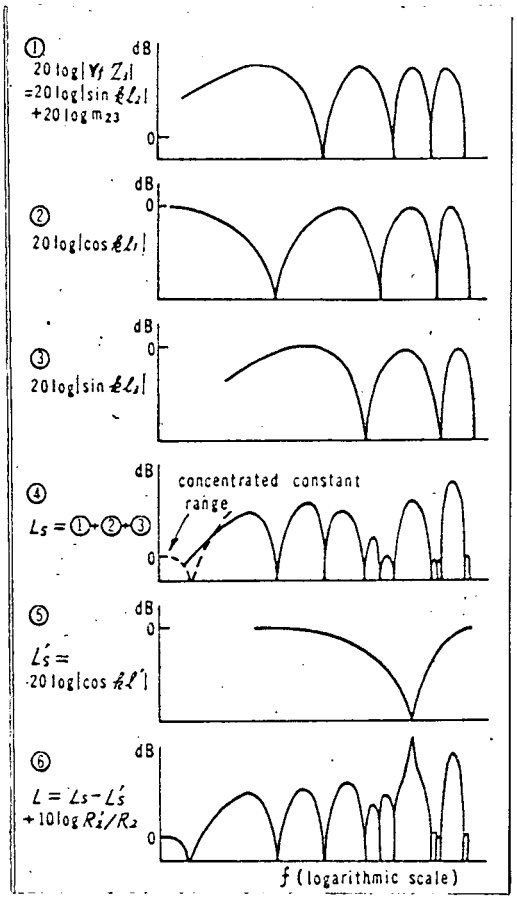

Figure 4. Procedure of graphical calculation of L (constant velocity source)

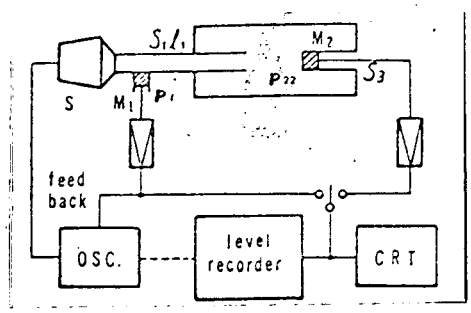

Figure 5. Schematic view of the measuring system of log $|Y_f Z_3|$. S: loudspeaker, M_1, M_2: microphone

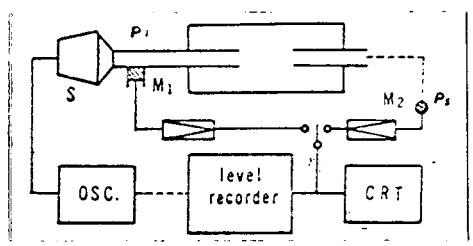

Figure 6. Schematic view of the measuring system of L. S: loudspeaker; M_1, M_2: microphone

The equipment shown in Figure 6 was used in the measurement of L. Giving due consideration to the S/N-ratio and distortion, the sound source was a 20-cm MFB-type speaker enclosed in a steel cabinet without the use of sound pressure feedback. The composite result was obtained graphically by using

$$L = (20\log|p_1'| - 20\log|p_s'|) - (20\log|p_1| - 20\log|p_s|) \tag{31}$$

and the recording of the sound pressure p_1' and p_s' at the input and at a given external location, respectively, without the muffler system, and of the sound pressure p_1 at the input and

the external pressure p_s at the same location with the muffler system. This approach is suitable for the case of a constant-pressure source.

6. Experiments

Examples of the comparison between the measured value and the graphically-synthesized results are shown in Figures 7 and 8 for a basic-type and an insert pipe type muffler system,

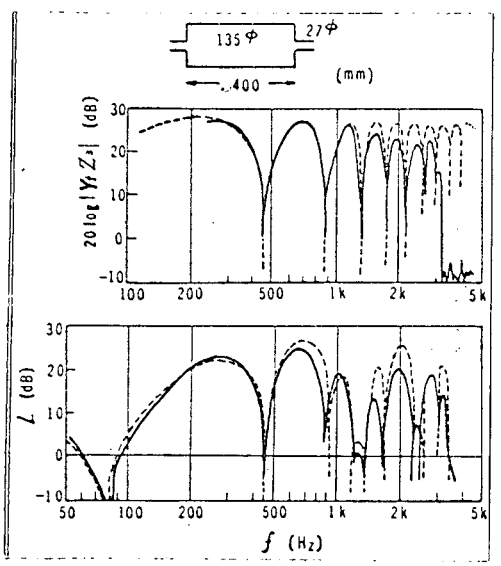

Figure 7. 20 log $|Y_f Z_3|$ of a basic type chamber and L of a muffler with this chamber (l_1 = 86.5 mm 27 mm φ, l_3 = 147.6 mm 27 mm φ and l_1' = 86.5 mm 27 mm φ). The solid curves show the results of measuring and the dotted curves show those by a graphical method

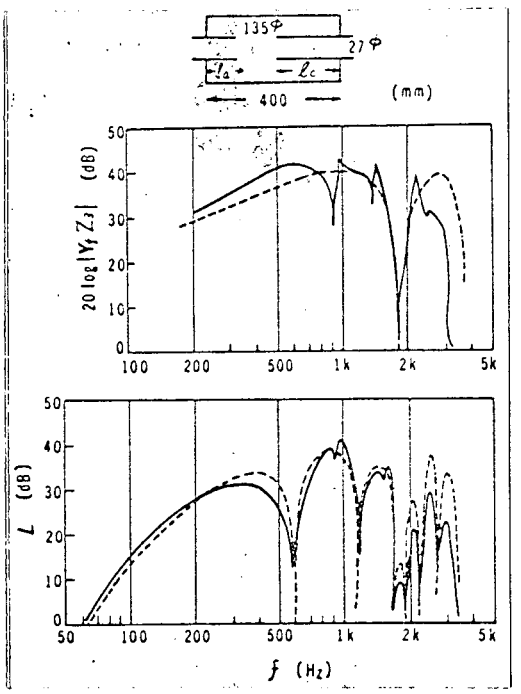

Figure 8. 20 log $|Y_f Z_3|$ of a insert pipe type chamber (l_a = 88 mm, l_c = 185 mm, real length), and L of a muffler with this chamber (l_1 = 173 mm 27 mm φ, l_3 = 337 mm 27 mm φ and l' = 173 mm 27 mm φ). The solid curves show the result of measuring and the dotted curves show those by a graphical method

respectively. Although in Figure 8 the calculation is shown for pipe insertion lengths of 1/2 and 1/4 of the chamber length, the actual length was considerably shorter. This is due to the fact that it was necessary to estimate the equivalent length of the chamber as being considerably longer than the actual length because of the approximation used for the mathematical expression [2, 6]. When this is taken into account, good agreement exists between the measured value and the calculated value for a not-too-high frequency range.

The measured value decreases rapidly with frequency above approximately 3 KHz. The cut-off frequency f_c measured for cylindrical chambers of various sizes is shown in Figure 9 [4], and agrees closely with the fundamental resonant frequency [5] /128

$$f_{r_1}=\frac{1.2197}{2a_2}c\ [\mathrm{Hz}] \qquad (32)$$

in the direction perpendicular to the axis of the cylinder with radius a_2. In the case of a rectangular cross section with width $2a_2$, the cutoff frequency becomes

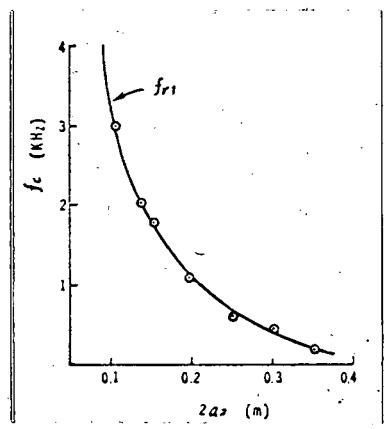

Figure 9. Cutoff frequency f_c of a cylindrical chamber of radius a_2

$$f_{r_1}=\frac{0.5}{2a_2}c\ [\mathrm{Hz}] \qquad (33)$$

That is, the assumption that the sound wave below this frequency is an axially-propagating wave is valid. Above this frequency, the muffler system cannot be effective without additional losses. Moreover, the plane wave hypothesis deteriorates and the peak of the graph decreases with frequency, even in the above-mentioned frequency range, when the placement of the input pipe or the tailpipe is not concentric with the

axis of the chamber, when the end surface of the chamber is not flat, or when S_1/S_2 is extremely large.

Furthermore, the muffler system acts as a resonant-type rather than an expansion-type system when the length of the chamber is so short that the longitudinal fundamental resonant frequency, $f_{i_1} = c/2l_2$ is smaller than the above-mentioned f_r, or when the insert pipe-type muffler is such that the outlet of the input pipe is extremely close to the inlet to the tailpipe [2, 6].

The error of the calculated values of L_s is large near the nulls because of the approximation used. However, in practice, losses that were theoretically neglected do exist, however minutely, because of such factors as the viscosity of the medium. The magnitude of the error near the nulls is determined by these losses. Because it is difficult to determine the losses precisely, and because the muffler system is ineffective in this range, it is appropriate to use the approximation if these factors are taken into account. /129

In order to carry out the separate and approximate analysis given in Figure 3, the magnitude of the tailpipe input impedance

$$Z_{31} \simeq j Z_3 \tan k l_3 \quad (34)$$

must be sufficiently large. In the range where $|\tan kl_3|$ is small, $|\sin kl_3|$ and, therefore L_s, are small and the system is ineffective. In the range where the system is effective, $|Z_{31}|$ is large, and the chamber outlet can be approximated by a closed outlet. Furthermore, when the tailpipe is extremely short or when the outlet is simply a hole in the end surface of the chamber, kl_3 is usually small, even in the frequency range below

f_{r_1}. In this case, the above-mentioned assumption does not apply, and the effectiveness of the muffler system is low, even in actual measurements.

7. Conclusion

In the above discussion, the behavior of the muffler system was investigated by considering the sound power radiating from the outlet. The effectiveness of the muffler system was calculated based on the assumption of no losses, a plane wave, and other assumptions for an expansion-type muffler system. Practical approximations were used, and it was shown that the properties of the chamber can be represented by 20 log $|Y_f Z_3|$.

Not only is the resultant expression very simple in form, the composite result can be easily obtained by graphical synthesis. Good agreement with the experimental value was shown by using a speaker as the sound source. Furthermore, from the comparison with the experimental value, the extent to which the plane wave assumption can be realized and the range of applicability of the mathematical expression became clear.

Because the properties of the system can be easily obtained by graphical synthesis, not only is the trouble of numerical calculation eliminated, but intuitive design is possible.

Moreover, because the value of 20 log $|Y_f Z_3|$ can be obtained through simple measurements, it is possible to easily understand the properties of rather complex chambers which are theoretically difficult to analyze.

Effects of the length of various parts of the muffler system, especially that of the tailpipe, can also be easily understood from the equation obtained above.

References

1. Japan Acoustic Material Society Publication. Noise Reduction Handbook. Gihodo, 1966, p. 375.

2. Okada. Method of Calculating Properties of Expansion-Type Muffler Systems. Electric Communication Society, Electric Acoustic Research Society Data, Acoustic 66, 1967, pp. 2 - 33.

3. Okada. Method of Calculating Properties of Expansion-Type Muffler Systems. Japan Acoustic Society, Lecture Dissertation Series, May 1967, p. 341.

4. Tsuji, Okada. On the Dimension Ratio of Cylindrical Chambers of the Filter-Type Muffler System. Japan Acoustic Society, Lecture Dissertation Series, October 1965, p. 293.

5. Morse, P. M. Vibration and Sound, 2nd Ed. McGraw-Hill, 1948, p. 399.

6. Okada and Yoshida. Approximate Calculation of the Properties of Filter-Type Muffler Systems in Terms of the Equivalent Open-Circuit Distributed Admittance (the Case of Insertpipe-Type Chamber). Japan Audio Society, Lecture Dissertation Series, November, 1966, p. 93.

Translated for National Aeronautics and Space Administration under contract No. NASw 2035, by SCITRAN, P. O. Box 5456, Santa Barbara, California, 93108